Biochimica et Biophysica Acta, 635 (1981) 267—283

BBA 48018

THE REACTION CENTER PROFILE STRUCTURE DERIVED FROM NEUTRON DIFFRACTION

JAMES M. PACHENCE [a,b,c], P. LESLIE DUTTON [b] and J. KENT BLASIE [a,b,c]

Departments of [a] Chemistry and [b] Biochemistry/Biophysics, University of Pennsylvania, Philadelphia, PA 19104 and [c] Brookhaven National Laboratory, Upton, NY 11973 (U.S.A.)

(Received June 24th, 1980)
(Revised manuscript received November 4th, 1980)

Key words: Neutron diffraction; Reaction center profile; Phosphatidylcholine bilayer; X-ray diffraction; Bacterial photosynthesis; (Rps. sphaeroides)

Summary

Both reaction center protein from the photosynthetic bacteria *Rhodopseudomonas sphaeroides* and egg phosphatidylcholine can be deuterium labelled; the reaction center protein can be incorporated into the phosphatidylcholine bilayers forming a homogeneous population of unilamellar vesicles. The lipid profile and the reaction center profile within these reconstituted membrane profiles were directly determined to 32 Å resolution using lamellar neutron diffraction from oriented membrane multilayers containing either deuterated or protonated reaction centers, and either deuterated or protonated phosphatidylcholine. The 32 Å resolution reaction center profile shows that the protein spans the membranes, and has an asymmetric mass distribution along the perpendicular to the membrane plane. These results were combined with previously described X-ray diffraction results in order to extend the resolution of the derived reaction center profile to 9 Å.

Introduction

The initial event in bacterial photosynthesis is the light-induced excitation of the reaction center bacteriochlorophyll special dimer, causing oxidation of the dimer and subsequent reduction of the iron-ubiquinone complex (formerly called the 'primary' acceptor, see Ref. 1). Knowledge of the organization of the active components in the reaction center protein within the membrane structure is essential for the understanding of the mechanism for the light-initiated electron transfer reactions involved in the primary events of bacterial photosynthesis and energy coupling. As a first step in the investigation of the structure

of the reaction center protein, X-ray diffraction studies were done on oriented multilayers of reconstituted reaction center-phosphatidylcholine membranes to determine the membrane electron-density profiles at various lipid/protein ratios [2]. Subtraction of an assumed lipid bilayer profile from the various membrane profiles resulted in a first order approximation to the protein profile which was consistent with the changes seen in the reconstituted membrane profile as a function of lipid/protein ratio. Since the lipid bilayer profile was based simply on the characteristics of the reconstituted membrane profiles at high lipid/protein ratios and the known composition of these membranes, the reaction center protein profile so derived cannot be considered unique.

The bacteria *Rhodopseudomonas sphaeroides* R26 mutant has been successfully cultured on a medium containing deuterium oxide [3]. In this paper, deuterated reaction center protein was isolated from such bacteria and subsequently re-incorporated into lipid bilayer membranes. The neutron scattering profiles derived for reconstituted membranes containing deuterated reaction centers are compared with those derived for membranes containing protonated reaction centers and used to directly obtain the 30 Å resolution reaction center protein profile by their difference. Similarly, we have obtained the lipid bilayer profile directly by comparing neutron scattering profiles for reaction center-phosphatidyl[$^2H_{13}$]choline versus reaction center-phosphatidylcholine membranes [4,5]. These results will be combined with previous X-ray diffraction studies [2] to obtain the reaction center molecular profile at 9 Å resolution.

Materials and Methods

Rhodopseudomonas sphaeroides R26 cells were grown in a mineral medium containing protonated succinate as the sole carbon source [6]; the bacteria were acclimated to a medium containing 95% ^2H_2O by gradual increase of ^2H_2O content at culture transfer [7]. Reaction centers were prepared after the method of Clayton and Wang [8], with an index of purity of 1.28 [2]. The degree of deuteration of the isolated reaction center protein was assayed in the following manner: (a) the protein was precipitated by chemical reduction of the detergent (lauryl dimethylamine oxide) with sodium dithionite [2]; (b) the pelleted protein was washed 3-times with 10 mM Tris-HCl, 1 mM sodium dithionite, pH 8.0, then was lyophilized and weighed; (c) the dry protein was oxidized with O_2 at a temperature of 200°C in a closed system. The concentration of H_2O was measured by NMR methods for both the protonated and deuterated protein samples. In addition, proton NMR spectra at 360 MHz of the deuterated reaction center protein in detergent showed only negligible absorption for aromatic protons in contrast to the protonated protein at the same concentration.

Egg phosphatidylcholine was isolated from fresh egg yolks according to the method developed by Singleton et al. [9], and assayed for purity via thin-layer and gas-liquid chromatography. The transphosphatidylation procedure used to label the phosphatidylcholine with ^2H was similar to the method described by Yang et al. [10], with minor modification. To achieve maximal incorporation of labelled choline, the time of the incubation, the amount of enzyme, and the amount of free choline was varied and the incorporation of [^3H]choline (10^5

cpm) per reaction mixture was measured. It was found that the optimal reaction mixture consisted of 1.5 μmol freshly isolated egg phosphatidylcholine, 110 μmol acetate, 50 μmol $CaCl_2$, 750 μmol [$^2H_{13}$]choline bromide (Merck) and 2 mg phospholipase D (Sigma), brought to a final volume of 2.1 ml with H_2O. To begin the reaction, 1.2 ml diethyl ether was added. The mixture was allowed to incubate for 30 min and the reacted phospholipids were then extracted from the reaction mixture with 4 ml diethyl ether/ethanol (4 : 1, v/v). After the solvents were evaporated, a fresh reaction mixture without phosphatidylcholine was added to the dried, reacted phospholipids and the transphosphatidylation reaction was repeated; it was found that one repetition was sufficient to optimize the incorporation. The phospholipids were again extracted, dried and dissolved in $CHCl_3$. Purification of phosphatidyl[$^2H_{13}$]-choline was done on a silicic acid column [11]. Silicic acid (approx. 10 g material/50 mg phospholipids) was prepared by (a) washing with $CHCl_3$ and allowing the excess solvent to evaporate; (b) heating the washed silicic acid to 140°C for 2 h followed by cooling to 20°C; (c) resuspending the cooled silicic acid in $CHCl_3$ and pouring the material into a 12 mm × 240 mm column, fitted with a glass filter. The sample was added with approx. 100 ml $CHCl_3$ and then washed with 125 ml $CHCl_3/CH_3OH$ (4 : 1, v/v). The phosphatidylcholine was eluted with $CHCl_3/CH_3OH$ (7 : 3, v/v). The phosphatidylcholine was assayed for purity by thin-layer chromatography on silica gel plates (Applied Sciences) and by measuring the oxidative index, A_{233nm}/A_{215nm} [12]. The average oxidative index over six phosphatidylcholine preparations was 0.143 (maximum 0.180). The hydrocarbon chain population was characterized by gas-liquid chromatography [13]. The concentration of phosphatidylcholine was measured by phosphate content by the method of Bartlett [14]. The yield of phosphatidylcholine from this procedure was approx. 20%; using a [^{3}H]choline tracer, it was found that 83% of the phosphatidylcholine contained labelled choline.

Phosphatidylcholine-reaction center membrane dispersions, and the subsequent partially dehydrated oriented membrane multilayers were formed according to Pachence et al. [2,15], using planar glass slides of the dimensions 10 mm × 20 mm as the multilayer substrate. After approx. 24 h of initial equilibration at 5°C in an atmosphere of 88% relative humidity (using a saturated KCl solution), the multilayer samples were placed in aluminum gas-tight canisters. The canisters were equipped with reservoirs for saturated salt solutions to maintain a specific relative humidity at a specific $H_2O/^2H_2O$ ratio during the experiment. The canisters fit into a temperature-regulated specimen chamber fixed on a goniometer mounted on the ω-axis of the Brookhaven low-angle diffractometer [16].

Neutron diffraction experiments were performed at the High Flux Beam Reactor at the Brookhaven National Laboratory, Upton, NY [16]. The monochromatic neutron beam (pyrolytic graphite crystal monochromator, $\Delta\lambda/\lambda = 0.025$) had a flux of 10^6—10^7 neutrons · cm^{-2} · s^{-1} at $\lambda = 2.36$ Å. The incident neutron beam flux was monitored by a low efficiency detector, so that the diffraction data could be corrected for fluctuations in the incident beam flux. The incident beam dimensions were fixed at 1 mm × 3 mm (width × hright) using adjustable slits on each end of a collimator (71.1 cm length), producing a full beam divergence of 0.161° impinging on the sample. The scattered neutrons

were detected on a two-dimensional position sensitive detector [17]. This detector has a spatial resolution of 1.5 mm in the meridional (horizontal) direction and 3.0 mm in the equatorial (vertical) direction, with a useable counting rate of 10^5 neutrons/s; therefore the meridional lamellar neutron diffraction from the oriented membrane multilayer was collected at intervals of $\Delta z^* = 0.00034$ Å^{-1} ($z^* = (2 \sin \theta)/\lambda$) for a typical specimen to detector distance of 1800 mm. A helium path is provided from the point of the specimen to the surface of the counter to minimize air scatter. Translocation of the multilayer into the beam and the determination of $\omega = 0°$ was achieved via ω-scans of the first-order lamellar reflection from a dipalmitoyl phosphatidylcholine multilayer (where ω is the angle of the incident beam with respect to the plane of the membrane multilayer). The lamellar diffraction data from the membrane multilayers were collected as a function of ω, with $0° \leqslant \omega \leqslant 2.5°$ and $\Delta\omega = 0.1°$. A diffraction data set from the two-dimensional detector was created for each ω-value and stored as an array of counts versus position along z (meridional) and y (equatorial) axes, which showed the extent and shape of each lamellar reflection for each ω-value. Since the oriented membrane multilayers have apppreciable mosaic spread (about 3° full width at half maximum for the phosphatidylcholine-reaction center system), lamellar reflections appear as arcs whose centers lie along the meridonal axis. As a first step in the data reduction, the total integrated lamellar diffraction was obtained as a function of z by summation along y over the maximal extent in y of the lamellar diffraction for each ω-value and subsequent summation over the entire range of ω-values (as shown in Fig. 1 where z has been converted to $z^* = (2 \sin \theta)/\lambda$).

A background scattering function was calculated for such total integrated lamellar diffraction data by fitting a smooth curve through the regions between lamellar reflections via a cubic spline fit algorithm [18] with the modification that the data was first subjected to consecutive double channel linear smoothing or Fourier filtering until the noise was essentially eliminated. The background scattering function generation from this smoothed data was subtracted from the unmodified data set (compare Figs. 1 and 3). A background scattering function was deemed reasonable if: (a) the average of the noise fluctuations between the lamellar reflections was approximately zero; (b) the centroids of the reflections did not shift from $z^* = h/D$ (where $h = 1, 2, \ldots h_{max}$ and D is the multilayer periodicity); and if (c) the background scattering functions were qualitatively similar to the scattering from a glass slide.

The structure factors were derived from the background corrected integrated lamellar neutron diffraction according to the equation:

$$F(h) = B \cdot a(h) \cdot L(h) \cdot e^{i\phi(h)} \cdot \sqrt{I(h)}$$

$I(h)$ is the integrated intensity of the h-th order lamellar reflection ($h = 1, 2, \ldots h_{max}$), where the integration in y was over the extent of the lamellar reflection, the integration in ω was over the range $(\theta_h - 0.6°) \leqslant \omega \leqslant (\theta_h + 0.6°)$ where $\omega = \theta_h$ is the Bragg angle for the h-th order reflection and the integration in z^* was over a range centered about $z^* = h/D$ for which the total integrated lamellar diffraction was greater than the background scattering. $L(h)$ is the Lorentz factor [19] (which is simply h), $a(h)$ is the neutron attenuation correction, $\phi(h)$ is the phase, and B is a scale factor between two data sets. The scale factor and

the phase assignment are discussed in the Results section. The attenuation correction is calculated according to $a(h) = \exp(\mu \cdot l(h))$ where μ is the linear absorption coefficient and $l(h)$ is the path length through the sample for a particular reflection h. For the range of Bragg angles ($0° \leqslant \theta_h \leqslant 2.5°$) and the thickness (20—60 μM) and diameter (1 cm) of the planar membrane multilayer utilized, $l(h)$ and hence the absorption correction is virtually independent of Bragg angle and can therefore be included in the overall constant B, which is the scale factor between different samples.

The neutron scattering contrast profiles for the multilayer unit cell were determined by the appropriate Fourier series according to Guinier [19]:

$$\rho(z) = 2/D \sum_{h=1}^{h_{max}} F(h) \cos(2\pi z h/D)$$

Results

A. Characterization of the lamellar neutron diffraction

Reaction centers isolated from *Rps. sphaeroides* R26 mutant which were grown on 95% ^2H_2O with a protonated carbon source were found to be more than 80% deuterated at the non-exchangeable positions. Model calculations based on the results of our earlier X-ray diffraction studies [2] indicated that the membrane multilayers consisting of deuterated reaction center protein and protonated phosphatidylcholine in 100% ^2H_2O should have a change in neutron scattering contrast by 35% over the membrane multilayers containing fully protonated components in 100% ^2H_2O; the average scattering length of the protonated protein is $1.87 \cdot 10^{-14}$ cm/Å^3 compared to $6.43 \cdot 10^{-14}$ cm/Å^3 for the deuterated protein [20]. Therefore, we expected that the lamellar neutron diffraction from the deuterated protein membrane multilayers would be significantly different from the diffraction from the fully protonated membrane multilayers. Similarly, upon substituting [$^2H_{13}$]choline for 83% of the protonated choline in phosphatidylcholine a change in contrast of approx. 8% was calculated. However, it should be noted that the change in scattering length occurs only at specific locations within the multilayer unit cell profile, and individual reflections can therefore be expected to change by as much as 30%. Indeed, there are significant differences between the lamellar neutron diffraction from the reconstituted membrane multilayers containing deuterated components and the membrane multilayers containing fully protonated components where the membranes are hydrated with ^2H_2O (see Figs. 3 and 4).

The logarithm of the lamellar neutron diffraction from the reconstituted membrane multilayers containing protonated and deuterated reaction centers is shown in Fig. 1 A and B, respectively. Four diffraction orders were observed, with the periodicity of this set of data being D = 128 Å. A second series of experiments were done to compare the lamellar neutron diffraction from reaction center-phosphatidyl[$^2H_{13}$]choline membranes with that from fully protonated membranes (Fig. 2). Again, four diffraction orders were observed, with the periodicity (D = 134 Å) being slightly greater than for the diffraction data of Fig. 1. The membrane multilayers were exposed to the neutron beam of $7 \cdot 10^5$ counts/s for approx. 8 h. The relative integrated values of the lamellar

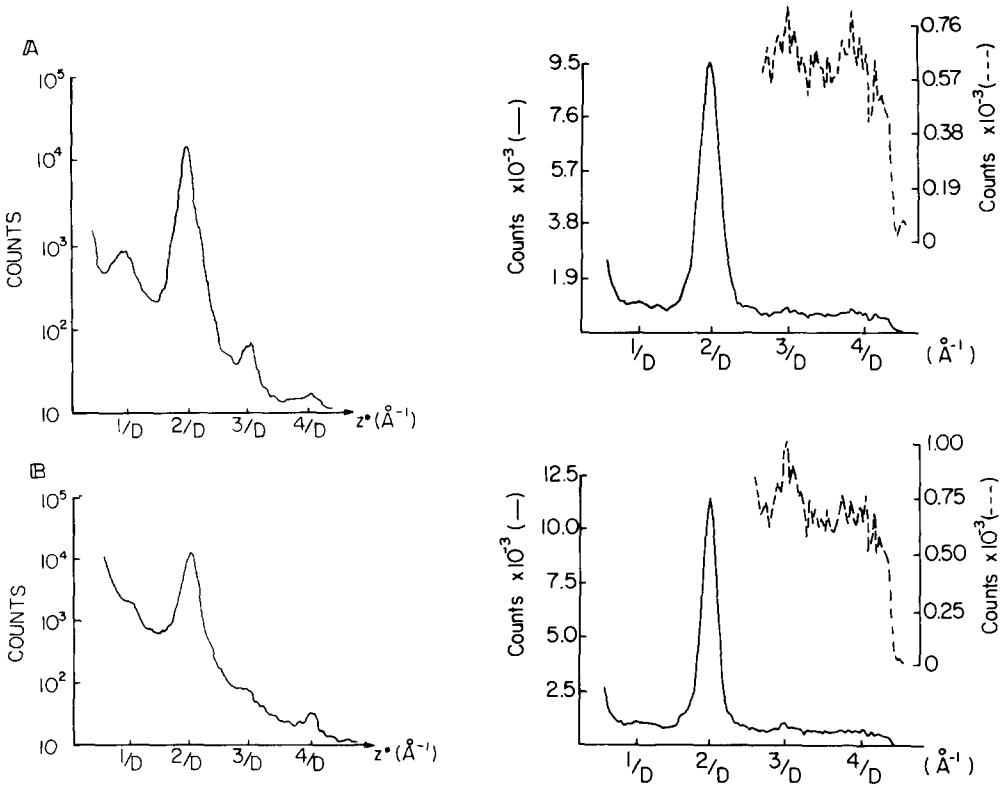

Fig. 1. Lamellar neutron diffraction pattern (log scale) from partially dehydrated oriented membrane multilayers consisting of (a) protonated reaction centers incorporated into egg phosphatidylcholine; and (b) deuterated reaction centers incorporated into egg phosphatidylcholine. The multilayer periodicity from (A) and (B) was D = 128 Å ± 0.5 Å. The membrane multilayers were subjected to an atmosphere of 88% relative humidity, at 100% ^2H_2O, with a temperature of 6°C. λ = 2.37 Å, $\Delta\lambda/\lambda$ = 0.025, and the incident beam flux was approximately $7 \cdot 10^5$ neutrons/s in 0.16° divergence.

Fig. 2. Lamellar neutron diffraction patterns from partially dehydrated oriented membrane multilayers consisting of (A) protonated reaction centers incorporated into phosphatidylcholine; and (B) protonated reaction centers incorporated into phosphatidyl[$^2H_{13}$]choline. The inset shows the weaker reflections on an expanded scale. The membrane multilayers were subjected to an atmosphere of 88% relative humidity at 100% ^2H_2O, with a temperature of 6°C. The multilayer periodicity from the patterns in A and B was D = 134 Å ± 0.8 Å.

reflections $I(h)$ after an 8 h exposure were not changed from those observed after only 2 h exposure.

The background-corrected lamellar neutron diffraction of Figs. 3 and 4 is characteristic for systems having two apposed membrane profiles per multilayer unit cell with a relatively low degree of asymmetry for the single membrane profile; the multilayer lattice periodicity D (128—134 Å) is more than twice that of the pure lipid multilayer (58 Å) and the integrated intensities of the odd order reflections are generally small compared to the even order reflections [21]. This observation supports earlier evidence which indicated that these membrane multilayers contain oriented stacks of flattened unilamellar vesicles which produces a unit cell profile containing the membrane pair profile of one flattened vesicle (see Refs. 2 and 21).

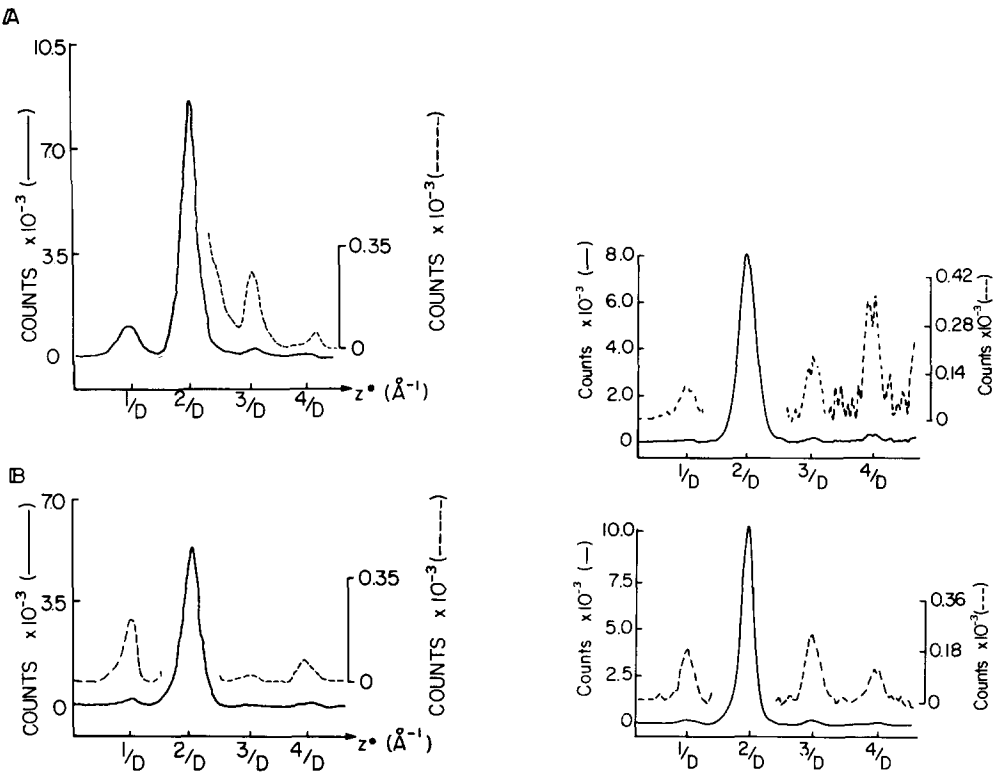

Fig. 3. Baseline corrected, numerically smoothed lamellar neutron diffraction patterns from oriented membrane multilayers of (A) protonated reaction center-protonated lipid; and (B) deuterated reaction center-protonated lipid. The inset shows the weaker reflections on an expanded scale. Conditions of the experiment are given in Fig. 1.

Fig. 4. Baseline corrected, numerically smoothed lamellar neutron diffraction from oriented membrane multilayers of (A) protonated reaction center protonated lipid; and (B) protonated reaction center-deuterated lipid. The inset shows the weaker reflections on an expanded scale. D = 134 Å ± 0.8 Å. Conditions of the experiment are given in Fig. 2.

Therefore, the multilayer unit cell profile is centrosymmetric and the phase assignment $\phi(h)$ for a particular integrated lamellar reflection, $I(h)$, is either 0 or π. Four lamellar reflections were recorded for each experiment corresponding to a resolution of approx. 32 Å in the unit cell profile; therefore, there are 2^4 possible phase combinations for each data set. However, only 2^3 combinations need to be investigated, as half of the phase combinations are related by an overall change in sign which results in simply inverting the profile from $\rho(x)$ to $-\rho(x)$. This ambiguity has a trivial solution in the case of neutron diffraction from membrane multilayers at a high ^2H_2O content since the large positive neutron scattering density of the water spaces must occur between the membrane profiles in the unit cell profile (Fig. 6).

The unit cell neutron scattering profiles were calculated via a standard Fourier synthesis [19] for all phase combinations of the integrated lamellar reflections for both the deuterated membranes and the protonated membrane hydrated at 88% relative humidity with 100% ^2H_2O and 80% ^2H_2O. The phases

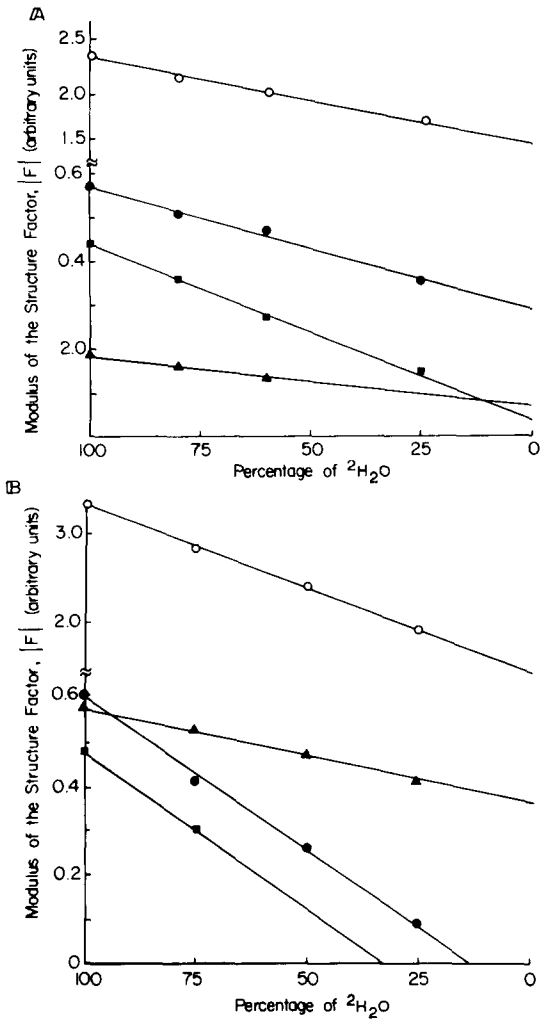

Fig. 5. The modulus of the structure factor, $|F(h)|$, is plotted versus the percentage of ^2H_2O of the membrane multilayer. Each reflection was integrated and corrected by the Lorentz factor. (A) Protonated reaction centers in phosphatidylcholine; and (B) deuterated reaction centers in phosphatidylcholine. ●———●, first reflection; ○———○, second reflection; ■———■, third reflection; ▲———▲, fourth reflection.

of the reflections $I(h)$ for both membranes did not change sign as the ^2H_2O concentration was changed over this range (Fig. 5). For a particular phase combination the corresponding unit cell water profile was calculated by taking the difference between the unit cell water profiles at the two ^2H_2O concentrations; therefore, eight possible unit cell water profiles were generated for both the deuterated and the protonated membranes. X-ray diffraction studies have shown that the deuterated and protonated proteins can be considered isomorphous with respect to the distribution of components in the membrane profile to 8 Å-resolution (data not shown); it is also reasonable to assume that the deuterated and protonated reaction centers have the same number of exchange-

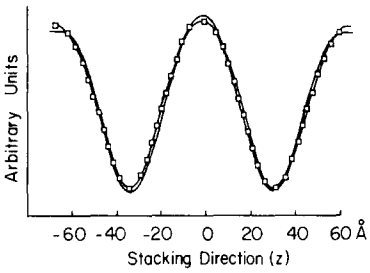

Fig. 6. The correct unit cell water space profile calculated from the lamellar diffraction from membrane multilayers at 88% relative humidity for both the protinated ($\rho_H^{^2H_2O}(x) - \rho_H^{H_2O}(x)$) (———) and deuterated protein ($\rho_{^2H}^{^2H_2O}(x) - \rho_{^2H}^{H_2O}(x)$) (□———□) cases. All possible phase combinations were used to generate eight possible water space profiles for each membrane. Since the water space profiles from membranes having protonated protein versus that having deuterated protein should superimpose, the correct phase assignment for the lamellar neutron diffraction data was obtained from the two water space profiles providing the best fit. One unit cell profile contains two apposed membrane profiles and hence three water spaces centered about the positions $z = 0$ Å and $|z| = D/2$.

able protons. Therefore, the unit cell water profiles for both deuterated and protonated membranes must be the same. As a direct consequence, the phase assignment for the lamellar neutron reflections was made by finding the phase combination for the membranes with deuterated components (whose unit cell profile is designated $\rho_{2_H}(x)$) and that for the membranes with protonated components (profile $\rho_H(x)$) which produced the best quantitative agreement for the two unit cell water profiles ($[\rho_H^{^2H_2O}(x) - \rho_H^{H_2O}(x) = \rho_{^2H}^{^2H_2O}(x) - \rho_{^2H}^{H_2O}(x)]$, Fig. 6). For each of the pairs of phase combinations, an overall scale factor was employed to compensate for the possible small differences in the amount of scattering material for two different membrane samples which minimized the agreement parameter R_0. Table I and II show the values of R_0 for the various pairs of phase combinations, and the corresponding scale factors, F_0. Note that for the pairs corresponding to the lowest value of R_0, the scale factors are closest to 1, which is to be expected since similar amounts of material were used to make each multilayer. We note that the differences between the two

TABLE I

FIT PARAMETERS BETWEEN ALL POSSIBLE WATER SPACE PROFILES FOR DEUTERATED AND PROTONATED REACTION CENTER-LIPID MEMBRANES

(The other comparisons of the two phase sets resulted in R_0 values which were greater than 0.35.)

Deuterated reaction centers in phosphatidylcholine	Protonated reaction centers in phosphatidylcholine	Chi-squared parameter R_0	Scale factor F_0
$\pi \cdot 0 \cdot 0 \cdot \pi$	$\pi \cdot 0 \cdot 0 \cdot 0$	0.107	0.973
$\pi \cdot 0 \cdot 0 \cdot \pi$	$\pi \cdot 0 \cdot 0 \cdot \pi$	0.117	0.879
$\pi \cdot 0 \cdot \pi \cdot \pi$	$\pi \cdot 0 \cdot \pi \cdot 0$	0.120	0.894
$\pi \cdot 0 \cdot 0 \cdot 0$	$\pi \cdot 0 \cdot 0 \cdot 0$	0.131	0.874
$\pi \cdot 0 \cdot \pi \cdot 0$	$\pi \cdot 0 \cdot \pi \cdot \pi$	0.208	0.859
$\pi \cdot 0 \cdot 0 \cdot 0$	$\pi \cdot 0 \cdot 0 \cdot \pi$	0.213	0.855
$\pi \cdot 0 \cdot \pi \cdot \pi$	$\pi \cdot 0 \cdot \pi \cdot \pi$	0.231	0.891
$\pi \cdot 0 \cdot \pi \cdot \pi$	$\pi \cdot 0 \cdot \pi \cdot 0$	0.240	0.900

TABLE II

FIT PARAMETERS BETWEEN ALL POSSIBLE WATER SPACE PROFILES REACTION CENTER-DEUTERATED LIPID MEMBRANES AND REACTION CENTER-PROTONATED LIPID MEMBRANES

(The other comparisons of the two phase sets resulted in R_0 values which were greater than 0.50.)

Reaction centers in deuterated lipid	Reaction centers in protonated lipid	Chi-squared parameter R_0	Scale factor F_0
$\pi \cdot 0 \cdot 0 \cdot \pi$	$\pi \cdot 0 \cdot 0 \cdot \pi$	0.119	0.737
$\pi \cdot 0 \cdot \pi \cdot 0$	$\pi \cdot 0 \cdot \pi \cdot 0$	0.141	0.825
$\pi \cdot 0 \cdot \pi \cdot \pi$	$\pi \cdot 0 \cdot \pi \cdot 0$	0.146	0.703
$\pi \cdot 0 \cdot 0 \cdot 0$	$\pi \cdot 0 \cdot 0 \cdot 0$	0.178	0.702
$\pi \cdot 0 \cdot 0 \cdot \pi$	$\pi \cdot 0 \cdot \pi \cdot 0$	0.181	0.737
$\pi \cdot 0 \cdot 0 \cdot \pi$	$\pi \cdot 0 \cdot 0 \cdot 0$	0.423	0.735
$\pi \cdot 0 \cdot 0 \cdot 0$	$\pi \cdot 0 \cdot 0 \cdot \pi$	0.478	0.750
$\pi \cdot 0 \cdot \pi \cdot 0$	$\pi \cdot 0 \cdot 0 \cdot 0$	0.486	0.745

smallest R_0 values in Tables I and II are significant considering that the counting statistics for the weakest integrated reflections were smaller by a factor of two; also the use of data smoothing routines for background scattering corrections reduces the possible errors due to noise fluctuations by at least one-half (we have assumed that the counting statistics of the weakest reflections produced greater systematic error than the background subtraction procedure). Therefore, the phase combination pair corresponding to the lowest value of R_0 was taken to be the correct phase solution to the particular set of lamellar reflection data (Table I and Table II).

B. Direct derivation of the protein profile

The correct unit cell neutron scattering density profiles for protonated reaction center-phosphatidylcholine membranes (Fig. 7A) and for deuterated reaction center-phosphatidylcholine membranes (Fig. 7B) show two membranes per unit cell, with the features being dominated by the high density ^2H_2O spaces centered about $x = 0$ Å and $|x| = 60$ Å and the low density lipid hydrocarbon cores of the two membranes centered about $|x| = 30$ Å. Using the scaling factors from Table I, the protonated protein-lipid membrane profile was subtracted from the deuterated protein-lipid membrane profile, to produce the reaction center protein * of Fig. 8 A. The scaling procedures used here places the deuterated and the protonated profiles on exactly the same relative scale. Therefore, within the error of the neutron diffraction data, the points about 0 Å and $\pm D/2$ Å of the unit cell contained no deuterated protein component. This protein profile was placed on an absolute neutron scattering density scale by using the average scattering density of the protein as calculated from the known chemical composition of the reaction center [23]. Furthermore, the protein density (g/cm^3) was used to calculate the area of the protein within different regions of the protein profile (left side of Fig. 8A). The total volume of 108 000 Å^3 of the protein as calculated from Fig. 8A is consistent with the

* In rigorous terms, the difference profile represents the profile distribution of non-exchangeable protein hydrogen atoms; assuming these hydrogen atoms to be uniformly distributed throughout the protein, this difference profile then represents the protein profile itself.

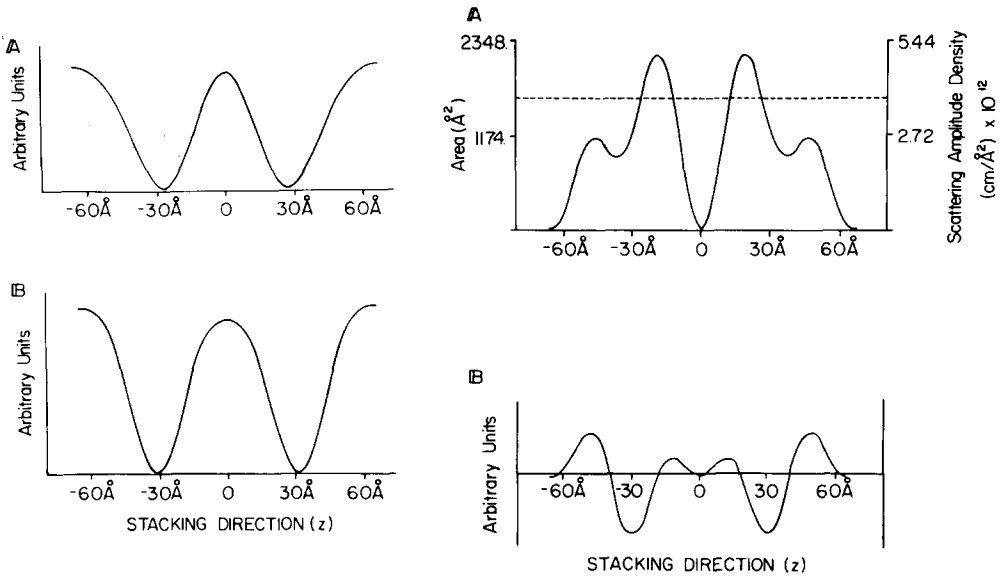

Fig. 7. The correct unit cell neutron scattering density profile (arbitrary scale) calculated from the lamellar neutron diffraction data from membrane multilayers consisting of (A) protonated reaction centers in phosphatidylcholine and (B) deuterated reaction centers in phosphatidylcholine. See Fig. 1 for the conditions of the experiment. The unit cell profile contains two apposed membrane profiles centered about the positions $|z| \sim 30$ Å.

Fig. 8. (A) One unit cell (two opposed membranes) of the reaction center protein profile is shown as area or neutron scattering density versus the stacking axis (z); this protein profile was calculated by subtracting the scaled protonated protein-lipid membrane profile (Fig. 7A) from the scaled deuterated protein-lipid membrane profile (Fig. 7B). (B) The lipid scattering density profile, shown on an arbitrary scale, was calculated by subtracting the water space profile (Fig. 6) and the protein profile (Fig. 8A) from the deuterated protein-lipid membrane profile of Fig. 7B, as described in the text.

volume of 98 500 Å^3 calculated from the Traube volumes of the reaction center amino acids [22]. This result confirms that the regions of the derived protein profile which are at zero-level to within experimental error in fact contain little or no protein.

Finally, the protein profile and the water profile can be subtracted from the membrane profile of Fig. 7B to determine the contribution of the phosphatidylcholine to the membrane profile. A scale factor between the water space profile and the membrane profile was derived so that the regions about $\pm D/2$ and 0 Å coincide for both profiles; the scaled membrane profiles from the X-ray diffraction experiments indicate that these are regions of pure water [2]. Further, the protein hydrogen-atom profile was previously scaled with the membrane profile as a direct consequence of the protein profile derivation. The scattering contribution due to protein atoms other than hydrogen can be calculated from the known amino acid content [23] and was added to the scaled protein hydrogen-atom profile; therefore, the scattering contribution due to protein and ^2H_2O was subtracted from the membrane profile to produce the lipid profile of Fig. 8B. The lipid profile derived in this way shows a difference between phospholipid head group densities on opposite sides of the membrane lipid bilayer,

which would contribute significantly to the asymmetry in the single membrane profile. This lipid profile can be directly determined experimentally utilizing a membrane containing deuterium-labelled lipid (next section), giving an independent verification of the so-derived lipid profile and consequently the reaction center protein profile.

C. Direct derivation of the lipid profile

The neutron diffraction data from Fig. 4 (from protein-deuterated lipid membrane versus protein-protonated lipid membrane multilayers) was phased according to the method outlined above, with the results given in Table II. The difference between the two lowest fit parameters is substantially greater than the counting statistics for the weakest integrated lamellar reflections, and therefore the phase set corresponding to the best fit of the water space profile pairs was taken to be correct. The difference profile (the scaled deuterated-minus the scaled protonated-lipid membrane profile) of Fig. 9 gives the profile distribution of the [$^2H_{13}$]choline label; however, the widths of the label peaks in this profile are resolution-limited. In order to obtain a more accurate description of the distribution of the label in the membrane profile, the difference profile was modelled using two Gaussian functions per membrane profile and refined against the experimental difference structure factors. Taking into account the experimental errors, these model calculations indicated that (a) there was 30% less label at the average head group position near $z = 0$ Å than at the position near $z = D/2$ which translates into a mole ratio for the two positions of 41 : 59 lipids, respectively, (b) the head group separation across the membrane profile was 41 ± 1 Å which agrees very well with that previously determined by X-ray diffraction [2] and (c) the characteristic ($1/e$) width of the distribution of head group labels near the position of $z = 0$ Å was in the range of 12 ± 2 Å while the width of the distribution near the position $z = D/2$ was more closely confined to 10 ± 0.5 Å; there are substantial differences between the calculated intensities and the experimental intensities (approximately factors of 10 for the weaker orders) whenever the characteristic width near $D/2$ was greater than the one near the origin.

It is important to note that the relative heights of the phospholipid head group maxima in the derived lipid profile (Fig. 8B) are virtually the same as

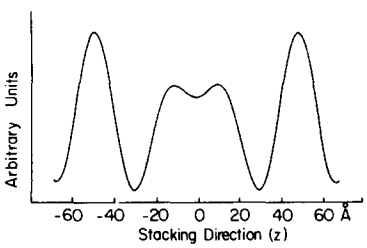

Fig. 9. One unit cell (two apposed membranes) of the difference profile for the protein-deuterated lipid membrane minus the protein-protonated lipid membrane is shown on an arbitrary scale versus the stacking axis (z). The data sets were scaled according to the method outlined in the text. The phosphatidylcholine was labelled in the polar head group ([$^2H_{13}$]choline), and this profile therefore characterizes the profile distribution of the head group label.

those in the head group label profile (Fig. 9). Within the accuracy of these experiments, these two independently derived lipid profiles are consistent and therefore firmly establish that the protein profile of Fig. 8A is correct.

Discussion

The deuterated reaction centers from *Rps. sphaeroides* can be considered structurally isomorphous and functionally similar to the protonated protein since: (1) it has been shown that bacteria grown on ^2H_2O or deuterated substrates do not exhibit major metabolic changes [3,7]; (2) the partially deuterated reaction centers displayed the same absorption spectrum and kinetic properties as the fully protonated proteins (Pachence, J.M., unpublished data); (3) the lamellar X-ray diffraction patterns from multilayers of deuterated reaction center-phosphatidylcholine membranes, measured to 8 Å resolution, was not significantly different from that previously reported [2] for protonated reaction center-phosphatidylcholine membranes (Pachence, J.M., unpublished data); and (4) measurements have shown that the orientations of the g-tensors with respect to the membrane plane for the EPR observable redox components were essentially identical for either deuterated or protonated reaction centers [31]. Therefore the changes which occur in the lamellar neutron diffraction as a result of the reconstituted membrane multilayers containing deuterated versus protonated reaction center protein can be considered to arise solely from the protein's profile structure.

As the vectorial distribution of the reaction centers in these reconstituted membranes was measured to be greater than 90% unidirectional (as determined by the oxidation of externally added cytochrome *c*, see Ref. 2), this protein profile should be considered as the profile structure of the reaction center molecule. Further, results from linear dichroism [21], EPR experiments [31], and cytochrome *c* oxidation kinetics [21,24] have verified that the orientation of the reaction center with respect to the membrane plane in the reconstituted membrane system is similar to the reaction center chromophore orientation in *Rps. sphaeroides* R26 chromatophore membranes [25]. This set of results suggests that the reaction center profile structure presented here is the same as the structure in vivo.

The reaction center molecule profile derived from these neutron diffraction experiments (Fig. 8A) is very similar to the protein profile derived from the earlier X-ray diffraction experiments (see Ref. 2). The most important feature to note is that the reaction center profile is highly asymmetric, with approx. 2/3 of its mass occurring within the inner half of the membrane profile facing the water space about $z = 0$ Å. The small discrepancies between the two reaction center profiles are due in part to the difference in experimental resolution.

The reaction center profile of Fig. 8A suggests that the distribution and configuration of the lipids on opposite sides of the membrane profile should be different in order to conform to the shape of the protein. We estimated the number of lipids displaced due to the area occupied by the reaction center from the calculated difference in area of the protein on one side of the membrane versus the other, using a value for the area/lipid of 57 Å [26]; we found that there must be a difference of at least 28% in the number of lipids on one side of the

membrane versus the other. Indeed, the lipid profile derived from the reaction center-phosphatidylcholine membrane profile (Fig. 8B) shows a marked asymmetry, as compared to pure lipid profiles (see Ref. 27). The lipid head group profile of Fig. 9 re-affirms experimentally that there must be a difference in the mole fraction of lipid components on opposite sides of the membrane; the difference in label distribution of 30% calculated from Fig. 9 is similar to the 28% calculated above. This difference is therefore a manifestation of the reaction center displacing more phosphatidylcholine on one side of membrane versus the other, and does not result from the possible curvature constraints imposed when forming the small membrane vesicles which are subsequently made into multilayers. Although the major contribution to the asymmetry in the derived lipid profile of Fig. 9 is the difference in the mole fraction of lipid on opposite sides of the membrane profile, the model analysis of the widths of the lipid polar head group regions suggests that the polar headgroups are more delocalized in the membrane profile on one surface (nearer z = 0 Å) than on the other; this effect also contributes to the asymmetric label distribution. However, either more accurate lower angle or higher angle lamellar neutron diffraction data will be needed to further characterize this second effect.

In our previous study [2] unit cell electron density profiles at 10 Å resolution were derived from lamellar X-ray diffraction of oriented reaction center-phosphatidylcholine membrane multilayers. An assumed lipid profile was subtracted from the protein-lipid profile to obtain a first approximation protein profile at 10 Å resolution. However, there was no experimental evidence for

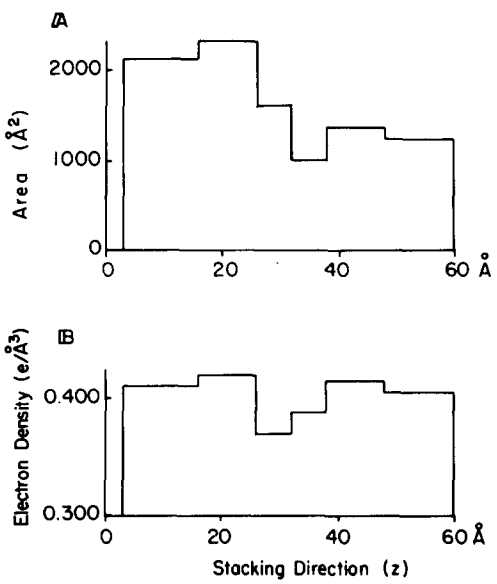

Fig. 10. A refined reaction center molecular profile obtained by subtracting the lipid electron density profile (calculated from the results obtained from Fig. 9; see text) from the 9 Å resolution protien-lipid membrane electron density profile derived from previous X-ray diffraction experiments (Ref. 2). One half of the unit cell, from the origin at 0 Å to $D/2$ is shown (equivalent to one membrane). (A) Area profile versus stacking axis (z), and (B) the electron density profile versus stacking axis (z). The refined profile was obtained under constraints dictated by the reaction center profile of Fig. 8A.

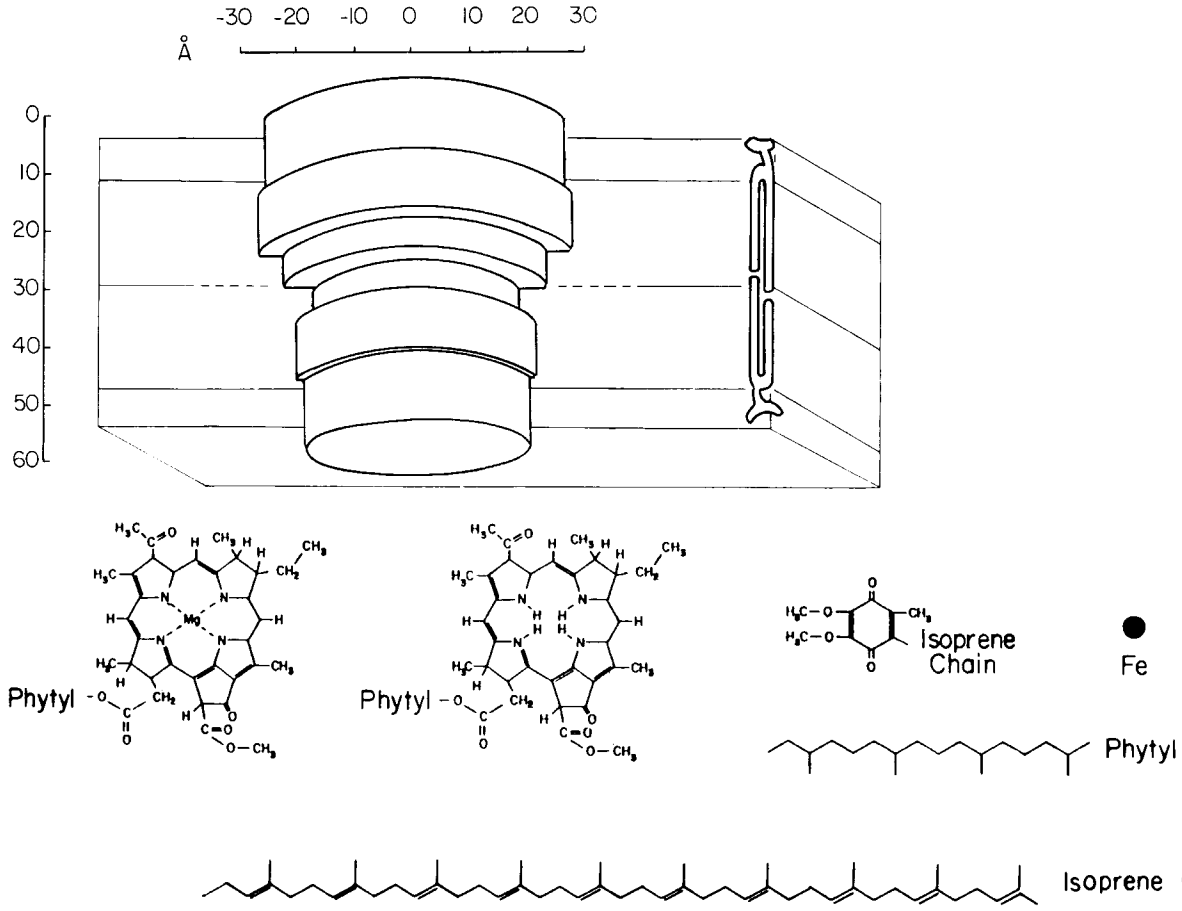

Fig. 11. Schematic representation of the cylindrically averaged reaction center protein within the reconstituted membrane. The reaction center consists of three subunits and contains four bacteriochlorophylls (BChl), two bacteriopheophytins (BPh), two ubiquinones (Q) and one iron atom. The arrangement of the three subunits within the reaction center must be consistent with this cylindrically averaged protein structure. The components important to electron transfer in the reaction center are shown, drawn to scale X2 with the membrane.

asymmetry of the lipid contribution profile when this first approximation to the protein profile was calculated. The present neutron diffraction study has directly measured the polar headgroup asymmetry in the lipid profile using deuterium labelled phosphatidylcholine in the reconstituted protein-lipid membranes. Based on the experimentally derived difference in the mole fraction of the lipid head group label on opposite sides of the membrane (Fig. 9), a revised 10 Å resolution lipid electron density profile was calculated; the symmetric 10 Å resolution egg phosphatidylcholine electron density profile derived from X-ray diffraction [2] was simply modified to include the asymmetry derived from the neutron experiments assuming that the average lipid conformation was the same on either side of the lipid bilayer. In the next step of the calculation, both the model lipid profile and the reaction center-lipid membrane profile were converted to their step function equivalents (see Ref. 2 for details of such a calculation). The step function equivalent to the modified 10 Å resolution lipid profile was then subtracted from the step function equivalent of the reaction center-lipid electron density profile (derived from the 10 Å resolution X-ray diffraction data) to produce the 10 Å resolution reaction center profile of Fig. 10. The scale on Fig. 10 was determined by equating the average of this profile to the average as derived by neutron diffraction (Fig. 8).

The asymmetric shape of the reaction center molecule in Fig. 10A would obviously displace more lipid on one side of the membrane bilayer than the other, and also this irregular shape of the protein might be expected to disrupt the normal packing of lipids differently within each monolayer; therefore, the derived lipid and protein profiles are consistent. Further, the electron density profile of the reaction center (Fig. 10B) indicates that the portion of the protein close to the center of the membrane has an electron density region that is significantly lower than the average density. As the reaction center is known to consist of three subunits [29], this low electron density region may indicate a point of subunit(s) contact (subunit contact within a non-polar environment would occur between the non-polar side chains of amino acids, producing a low electron density regions [30]).

The combined results from the neutron and X-ray diffraction experiments, shown in Fig. 10 were converted to a schematic representation of the cylindrically averaged reaction center molecule (averaged about the axis-perpendicular to the membrane plane) within the reconstituted membrane (Fig. 11). The diameter dimensions at the top were derived directly from Fig. 10. The arrangement of the three subunits within the reaction center must be consistent with this cylindrically averaged reaction center structure. The components important to electron transfer within the reaction center (four bacteriochlorophylls, two bacteriopheophytins, two ubiquinones, and one iron atom) are drawn to scale ×2 in Fig. 11, for comparison with the architecture of the reaction center-lipid membrane; experiments designed to locate the positions of the subunits and these components in the protein profile are currently in progress.

Acknowledgments

We would like to acknowledge the contributions of Dr. Benno Schoenborn of Brookhaven National Laboratory, in developing the neutron diffraction

experiments. We are also indebted to Heather Bonner and Susan Samuels for their technical assistance and to Peggi Mosley for preparing the manuscript. The work was supported by a grant from the United States Public Health Service GM 27309, and J.M.P. acknowledges his support from the Biomedical Research Support Grant, RR05415-16.

References

1 Dutton, P.L., Prince, R.C., Tiede, D.M., Petty, K.M., Kaufmann, K.J., Netzel, T.L. and Rentzepis, P.M. (1976) Brookhaven Symp. Biol. 28, 213—237
2 Pachence, J.M., Dutton, P.L. and Blasie, J.K. (1979) Biochim. Biophys. Acta 549, 348—373
3 Kohl, D., Townsend, J., Commoner, B., Crespi, H., Dougherty, R. and Katz, J. (1965) Nature 206, 1106—1110
4 Worcester, D.L. (1975) Brookhaven Symp. Biol. 27, III37—III57
5 Schoenborn, B.P. and Blasie, J.K. (1975) 5th International Biophysics (Congress, Villadsen and Christensen, Copenhagen, pp. 1379—1380
6 Dutton, P.L., Petty, K.M., Bonner, H.S. and Morse, S.D. (1975) Biochim. Biophys. Acta 387, 536—556
7 Lueking, D.R., Frailey, R.T. and Kaplan, S. (1978) J. Biol. Chem. 253, 451—457
8 Clayton, R.K. and Wang, R.T. (1971) Methods Enzymol. 23, 696—704
9 Singleton, W.S., Gray, M.S., Brown, M.L. and White, J.L. (1965) J. Am. Oil. Chem. Soc. 42, 53—63
10 Yang, S.F., Freer, S. and Benson, A.A. (1967) J. Biol. Chem. 242, 477—484
11 Rhodes, D.N. and Lea, C.H. (1957) Biochem. J. 65, 526—531
12 Klein, R.A. (1970) Biochim. Biophys. Acta 210, 486—489
13 Horwitz, A.F., Wragiht, A., Ludwig, P. and Cornell, R. (1978) J. Cell Biol. 77, 334—357
14 Bartlett, G.R. (1959) J. Biol. Chem. 234, 466—468
15 Pachence, J.M., Dutton, P.L. and Blasie, J.K. (1978) Biophys. J. 18, 9a
16 Schoenborn, B.P. and Nunes, A.C. (1972) Annu. Rev. Biophys. Bioeng. 1, 529—552
17 Alberi, J., Fischer, J., Radeka, N., Rogers, L.C. and Schoenborn, B.P. (1975) Trans. IEEE, Nuclear Science N522, 255—265
18 Conte, S.D. and de Boor, C. (1972) Elementary Numerical Analysis, pp. 233—240, McGraw-Hill, New York
19 Guinier, A. (1963) X-ray Diffraction, W.H. Freeman, San Francisco, CA
20 Yeager, M.J. (1975) Brookhaven Symp. Biol. 27, III3—III35
21 Pachence, J.M. (1980) Ph.D. Thesis, University of Pennsylvania
22 Cohn, E.J. and Edsall, J.T. (1943) Proteins, Amino acids and Peptides, Reinhold, New York
23 Steiner, L.A., Okamura, M.Y., Lopes, A.D., Moskowitz, E. and Feher, G. (1974) Biochemistry 13, 1403—1410
24 Pachence, J.M., Moser, C.C., Blasie, J.K. and Dutton, P.L. (1979) Biophys. K. 22, 55a (Abstr.)
25 Vermeglio, A. and Clayton, R.K. (1976) Biochim. Biophys. Biophys. Acta 449, 500—515
26 Tardieu, A., Luzzati, V. and Reman, F.C. (1973) J. Mol. Biol. 75, 711—733
27 Levine, J.K. and Wilkins, M.H.F. (1971) Nature New Biol. 230, 69—72
28 Blaurock, A.E. (1972) Adv. Exp. Med. Biol. 24, 53—63
29 Okamura, M.Y., Steiner, L.A. and Feher, G. (1974) Biochemistry 13, 1394—1402
30 Neurath, H., Hill, R.L. and Boeder, C.L. (1977) The Proteins, pp. 404—572, Academic Press, New York
31 Tiede, D.M., Leigh, J.S. and Dutton, P.L. (1980) Fed. Proc. 39, 1800 (Abstr.)